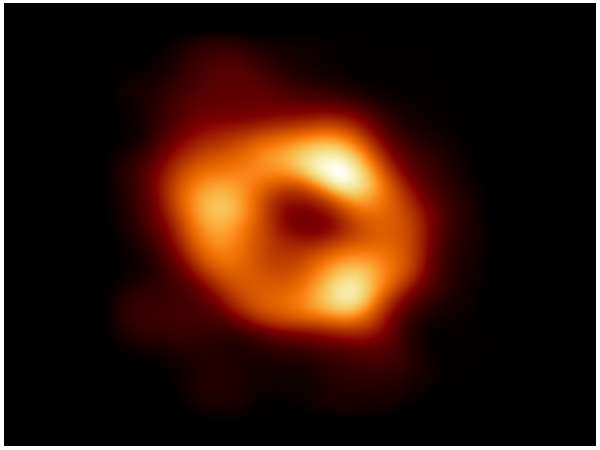

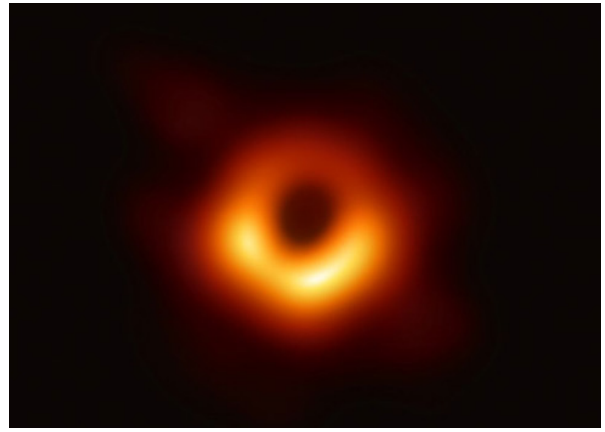

Finding the valid gravity theory from observations of black hole images

Vyacheslav Ivanovich Dokuchaev

Institute for Nuclear Research of the Russian Academy of Sciences

Lomonosov–2025, Moscow State University, Russia

Main Statements:

Observations of black hole images opens unique possibility for verification (or falsification) of modified gravity theories in the strong field limit when gravitation dominates over astrophysical factors.

Verification of modified gravity theories is crucial for physical interpretation of astrophysical and cosmological observations of the Universe and for understanding the physical origin of enigmatic dark matter and dark energy.

Visual images of supermassive black holes M87* and SgrA* have been observed recently by the collaboration Event Horizon Telescope.

Scrutinizing the modified gravity theories would be possible after construction of the Space Millimetron Observatory with nano-arcsecond angular resolution.

Shapes of black hole images depend on the distribution of emitting matter around black holes

Astrophysical Case 1 :

Radiation outside photon spheres

Luminous stationary background behind the black hole, which is a capture photon cross-section in the black hole gravitational field

Classical black hole shadow is viewed (J.M.Bardeen)

Astrophysical Case 2 :

Radiation inside photon spheres

Luminous accretion inflow near black hole event horizon

Event horizon shadow is viewed,

which is a lensed image of the event horizon globe

Astrophysical Case 1 : Classical black hole shadow

Stationary background outside photon spheres $r_{\rm ph} = const$

magenta region on the celestial sphere — classical black hole shadow (capture photon cross-section in the black hole gravitational field)

blue disk — Euclidean image of the event horizon (without gravity)

multi-colored curves — numerically calculated photon trajectories

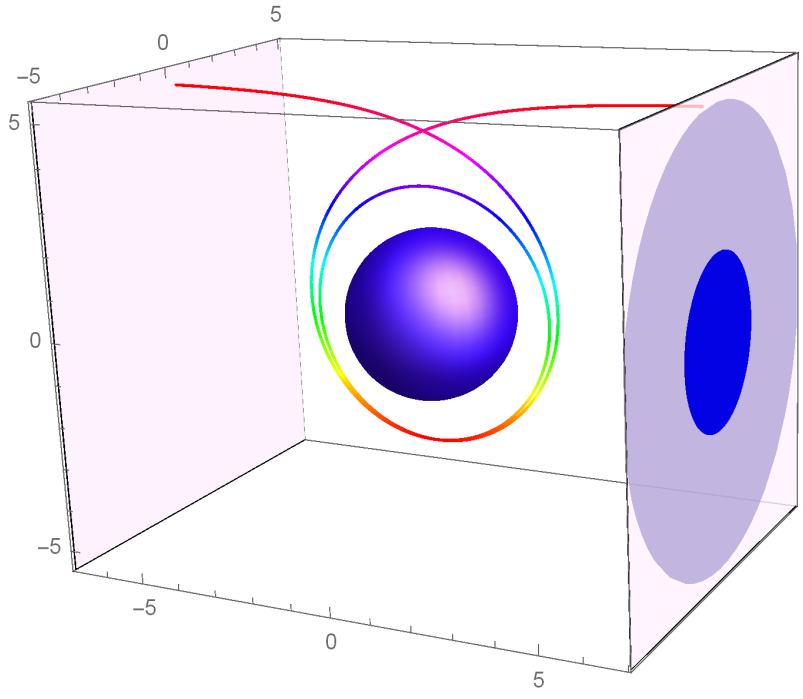

Schwarzschild

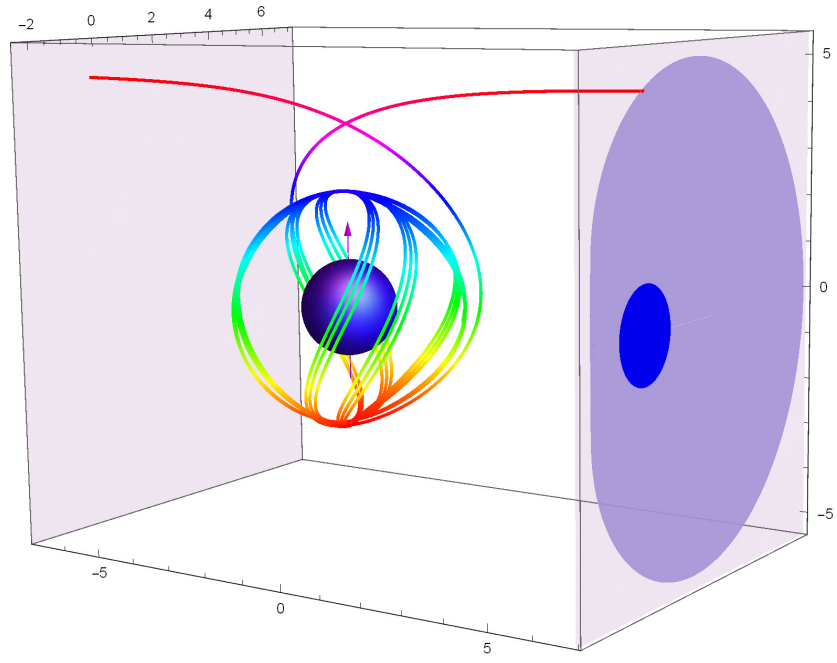

Kerr (near extreme)

Astrophysical Case 1 : Classical black hole shadow

Contour (boundary) of the black hole shadow on the bright background

Radiation outside the photon spheres $r_{\rm ph}$

Distant observer is in the black hole equatorial plane

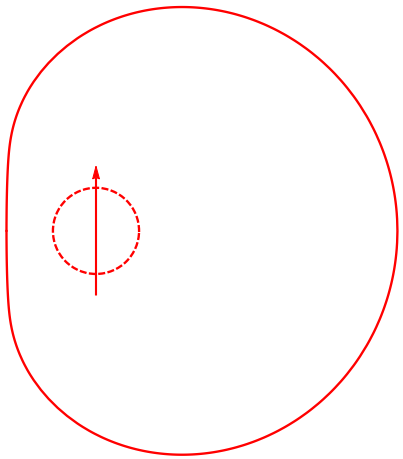

$a = 1$

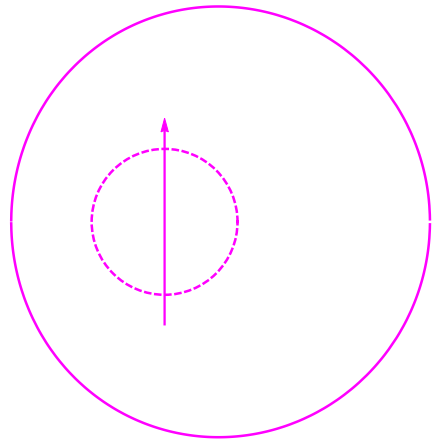

$a = 0.65$

Parametric equation for black hole shadow: $(\lambda, Q) = (\lambda(r), Q(r))$:

$$\lambda = \frac{(3-r)r^2 - a^2(r+1)}{a(r-1)}, \quad q^2 = \frac{r^3[4a^2 - r(r-3)^2]}{a^2(r-1)^2}$$

Bardeen 1973, Chandrasekhar 1983

λ — horizontal and $q = \sqrt{Q}$ — vertical photon impact parameters,

Q — Carter constant, arrow — black hole rotation axis

dashed circle — black hole event horizon $r_{\rm h} = (1 + \sqrt{1 - a^2})$

Two parameters for null geodesics: $\lambda = \Phi/E,\ q = Q^{1/2}/E$

Horizontal α **and vertical** β **impact parameters on the celestial sphere with a distant observer placed at the polar angle** θ_0**:**

$$\alpha = -\frac{\lambda}{\sin\theta_0}, \qquad \beta = q + a^2\cos^2\theta_0 - \lambda^2\cot^2\theta_0$$

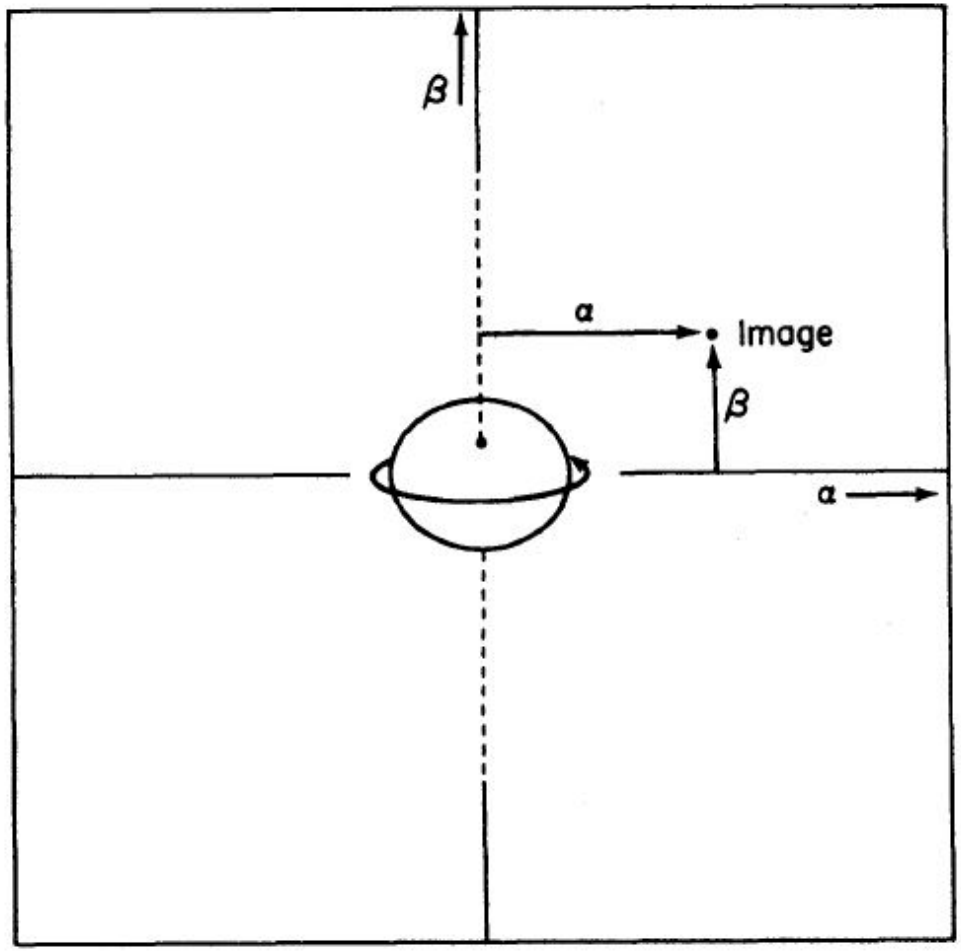

Kerr-Newman metric in the Boyer-Lindquist coordinate system (t, r, θ, φ)

$$ds^2 = \frac{\rho^2 \Delta}{\mathcal{A}} dt^2 - \frac{\mathcal{A} \sin^2\theta}{\rho^2}(d\varphi - \omega dt)^2 - \frac{\rho^2}{\Delta} dr^2 - \rho^2 d\theta^2$$

Potential $\quad A = e\rho^{-2} r(du - a\sin^2\theta d\varphi), \quad u = t + r, \quad F = 2dA$

$\rho^2 = r^2 + a^2\cos^2\theta$, $\Delta = r^2 - 2r + a^2 + e^2$, $\mathcal{A} = (r^2+a^2)^2 - a^2\Delta\sin^2\theta$

Metric 'angular velocity'

$$\boxed{\omega = (2Mr - e^2)\frac{a}{\mathcal{A}}}$$

Horizons: $\Delta = 0$, $r_\pm = 1 \pm \sqrt{1 - a^2 - e^2}$

R-regions $(\Delta > 0)$: $r > r_+$, $\qquad 0 < r < r_- < r_+$

T-region $(\Delta < 0)$: $r_- < r < r_+$

Locally Nonrotating Frame (LNRF):

$r = const$, $\theta = const$, $\varphi_0 = \omega t + const$ $\qquad$ J. M. Bardeen 1970

Equations of motion of a test particle B. Carter 1968

$$\frac{D^2 x^i}{D\tau^2} = \frac{\epsilon}{\mu} F^i_k \frac{Dx^k}{D\tau}$$

Lagrangian: $\frac{1}{2} g_{ij} \dot{x}^i \dot{x}^j + \epsilon A_i \dot{x}^i$

$(\dot{})$ — derivative with respect to an affine parameter λ

Normalization to the proper time: $\tau = \mu\lambda \quad \Longleftrightarrow \quad g_{ij} \dot{x}^i \dot{x}^j = -\mu^2$

Momenta: $p_i = g_{ij} \dot{x}^j + \epsilon A_i$

Hamiltonian: $H = \frac{1}{2} g^{ij} (p_i - \epsilon A_i)(p_j - \epsilon A_j) \quad \Rightarrow \quad H = -\frac{1}{2}\mu^2$

From the symmetries: $p_u = -E, \; p_\varphi = \Phi$

Three first integrals of motion: $p_u = -E, \; p_\varphi = \Phi, \; \mu = const$

A fourth first integral of motion is needed!

Advantage of the unexpected fact:

The Hamilton-Jacobi equation can be solved by separation of variables in the special coordinate system!

$$\frac{\partial S}{\partial \lambda} = \frac{1}{2} g^{ij} \left[\frac{\partial S}{\partial x^i} - \epsilon A_i \right] \left[\frac{\partial S}{\partial x^j} - \epsilon A_j \right]$$

Equations of motion of test particles B. Carter 1968

The Hamilton-Jacobi equation for the Jacobi action S

$$\frac{\partial S}{\partial \lambda} = \frac{1}{2} g^{ij} \left[\frac{\partial S}{\partial x^i} - \epsilon A_i \right] \left[\frac{\partial S}{\partial x^j} - \epsilon A_j \right]$$

If there is a separable solution:

$$S = -\frac{1}{2}\mu^2 \lambda - Eu + \Phi\varphi + S_\theta + S_r$$

$$p_\theta = \frac{\partial S}{\partial \theta}, \quad p_r = \frac{\partial S}{\partial r}$$

$$p_\theta^2 + \left(aE \sin\theta + \frac{\Phi}{\sin\theta} \right)^2 + a^2 \mu^2 \cos^2\theta =$$

$$= \Delta p_r^2 - 2[(r^2 + a^2)E - a\Phi + \epsilon e r] p_r + \mu^2 r^2 \quad \Rightarrow \quad = \mathcal{K} = const$$

$$p_\theta = \frac{dS}{d\theta} = \sqrt{V_\theta}, \quad p_r = \frac{dS}{d\theta} = \frac{1}{\Delta}\sqrt{V_r}, \qquad \Delta = r^2 - 2r + a^2 + e^2$$

Equations of motion for test particles B. Carter 1968

$$S = \frac{1}{2}\mu^2\tau - Et + \Phi\varphi + \int^{\theta} \sqrt{V_\theta}\, d\theta + \int^{r} \frac{\sqrt{V_r}}{\Delta} dr$$

$$V_\theta = Q + a^2(E^2 - \mu^2)\cos^2\theta - \Phi^2\cot^2\theta, \qquad \Delta = r^2 - 2r + a^2 + e^2$$

$$V_r = r[r(r^2 + a^2) + 2a^2]E^2 - 4arE\Phi - (r^2 - 2r)\Phi^2 - \Delta(r^2\mu^2 + Q)$$

$$\int^{r} \frac{dr}{\sqrt{V_r}} = \int^{\theta} \frac{d\theta}{\sqrt{V_\theta}}, \qquad \tau = \int^{\theta} \frac{a^2\cos^2}{\sqrt{V_\theta}} d\theta + \int^{r} \frac{r^2}{\sqrt{V_r}} dr$$

$$t = \int^{\theta} \frac{a^2E^2\cos^2\theta}{\sqrt{V_\theta}} d\theta + \int^{r} \frac{r^2(r^2 + a^2)E + 2ar(aE - \Phi)}{\Delta\sqrt{V_r}} dr$$

$$\varphi = \int^{\theta} \frac{\Phi\cot^2\theta}{\sqrt{V_\theta}} d\theta + \int^{r} \frac{r^2\Phi + 2ar(aE - \Phi)}{\Delta\sqrt{V_r}} dr$$

Andrew Strominger arXiv:1710.11112

Path integral equations of motion C. T. Cunninghan, J. M. Bardeen 1973

$$\int^{\theta} \frac{d\theta}{\sqrt{V_\theta}} = \int^{r} \frac{dr}{\sqrt{V_r}}, \quad V_\theta(\theta_{\min}) = 0, \quad V_r(r_{\min}) = 0$$

The integrals are understood to be path integrals along the trajectory

Integral equation with respect to $\lambda = \Phi/E$ and $q = Q^{1/2}/E$ for the trajectories of the first light echo:

$$\int_{\theta_s}^{\theta_{\max}} \frac{d\theta}{\sqrt{V_\theta}} + \int_{\theta_{\min}}^{\theta_{\max}} \frac{d\theta}{\sqrt{V_\theta}} + \int_{\theta_0}^{\theta_{\min}} \frac{d\theta}{\sqrt{V_\theta}} = \int_{r_s}^{r_{\min}} \frac{dr}{\sqrt{V_r}} + \int_{r_{\min}}^{r_0} \frac{dr}{\sqrt{V_r}}$$

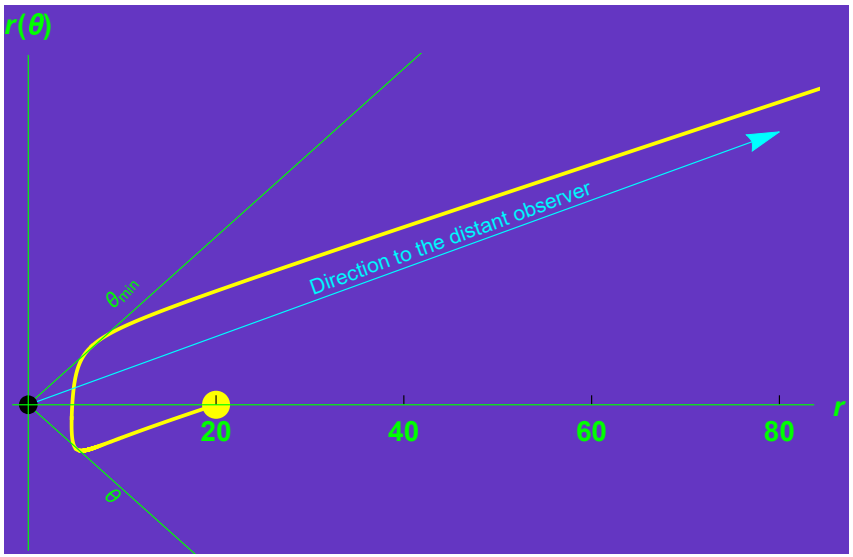

2D photon trajectory $r(\theta)$

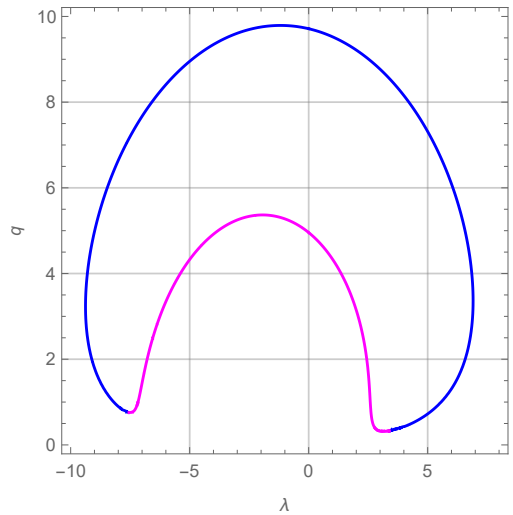

Solutions (λ, q)

Astrophysical Case 2 : GRMHD accretion simulations!!!

Accretion disk is very luminous at vicinity of event horizon!

Radiation from both the outside and inside photon spheres $r_{\rm ph} = const$

The Blandford-Znajek (1977) process (quite different from the α-disk!) is a suitable model for the General Relativistic Magnetohydrodynamics (GRMHD) accretion onto black holes, in which the inflowing plasma is strongly heated even in the vicinity of event horizon by the radial electric current and Poynting energy flux:

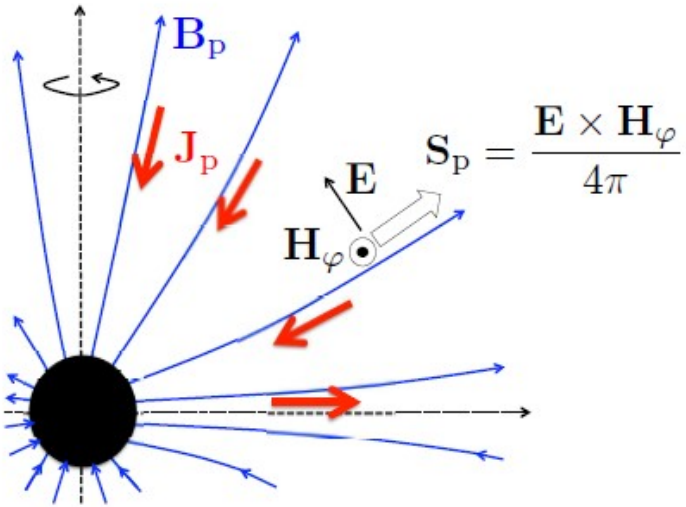

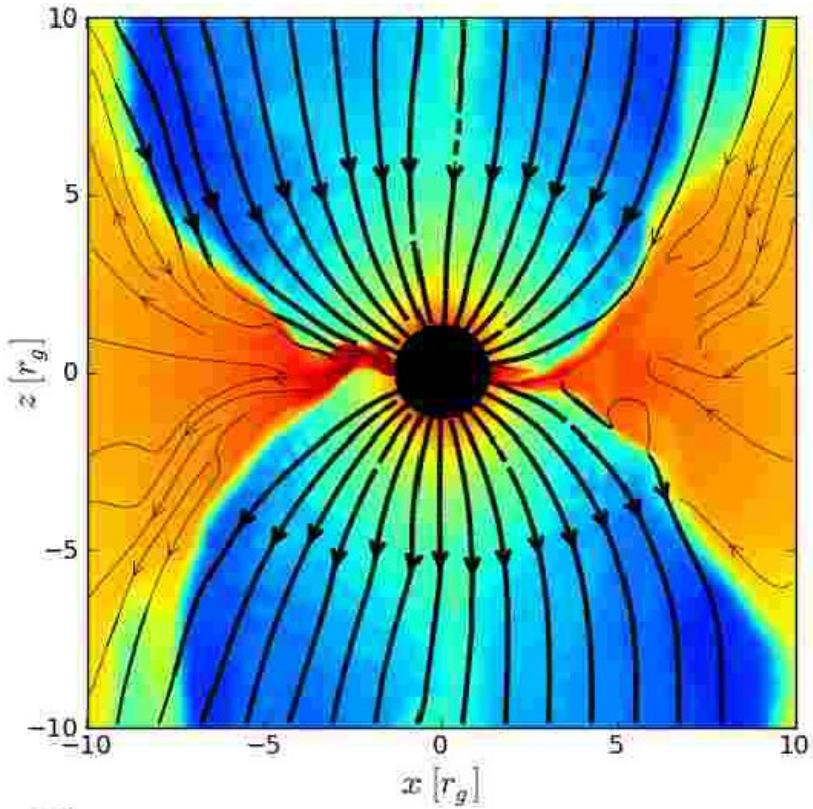

J.C.McKinney, A.Tchekhovskoy, R.D.Blandford (2012)

SgrA*, $a = 0.9982$: outgoing photons from $r = 1.01 r_{\mathrm{h}}$

Gravitationally lensed black hole event horizon globe is viewed from all sides!

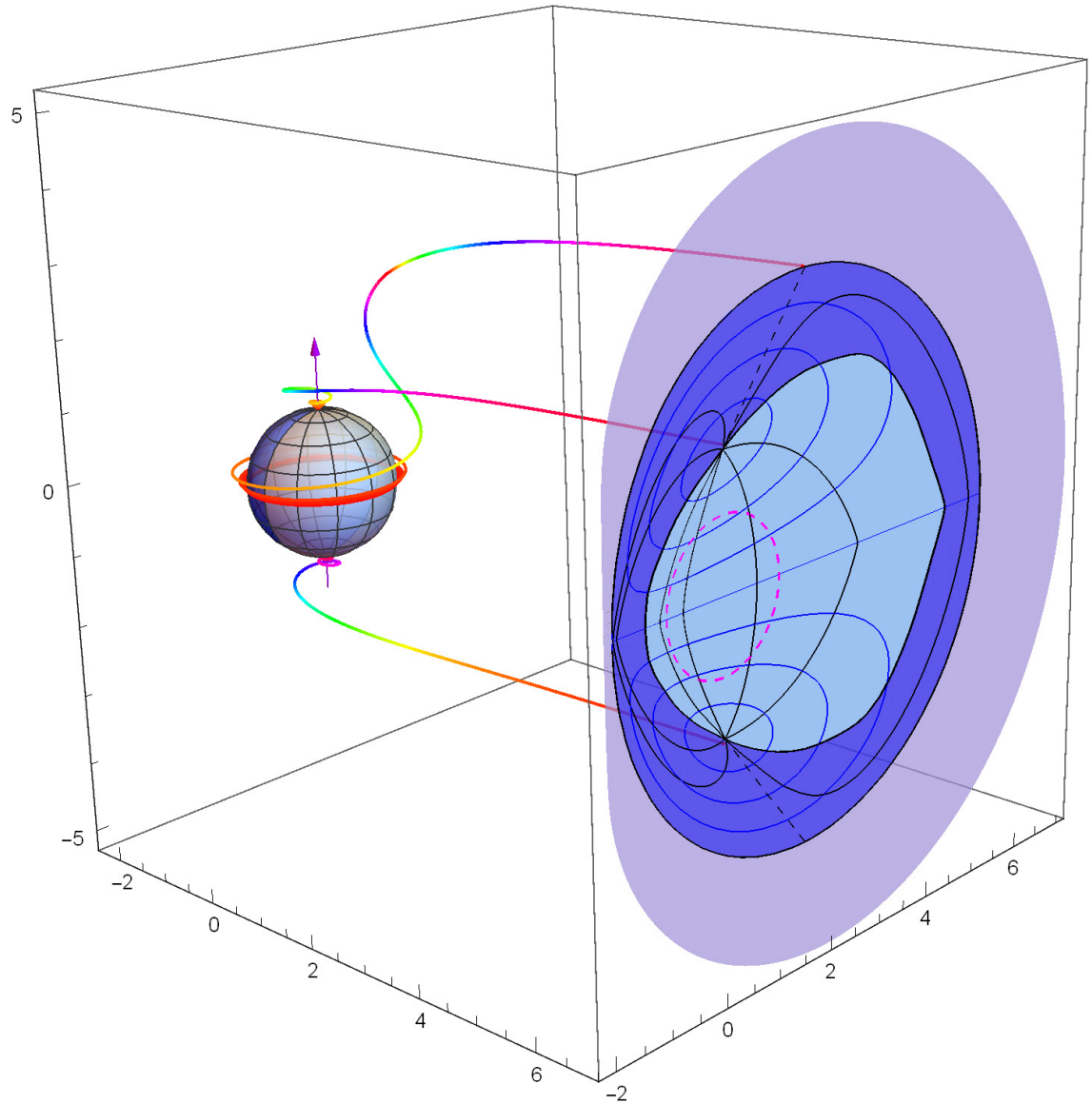

SgrA* Astrophysical Case 2 : Outgoing photon from

$r = 1.01 r_{\rm h}$

Radiation inside the photon spheres $r_{\rm ph}$

SgrA*, $a = 0.9982$, $\theta_0 = 82.2°$: dark spot (black region) is recovered by emission of the nonstationary inner part of thin accretion disk adjoining the event horizon in the black hole equatorial plane.

Photon trajectory with impact parameters $\lambda = -1.493$ and $q = 3.629$:

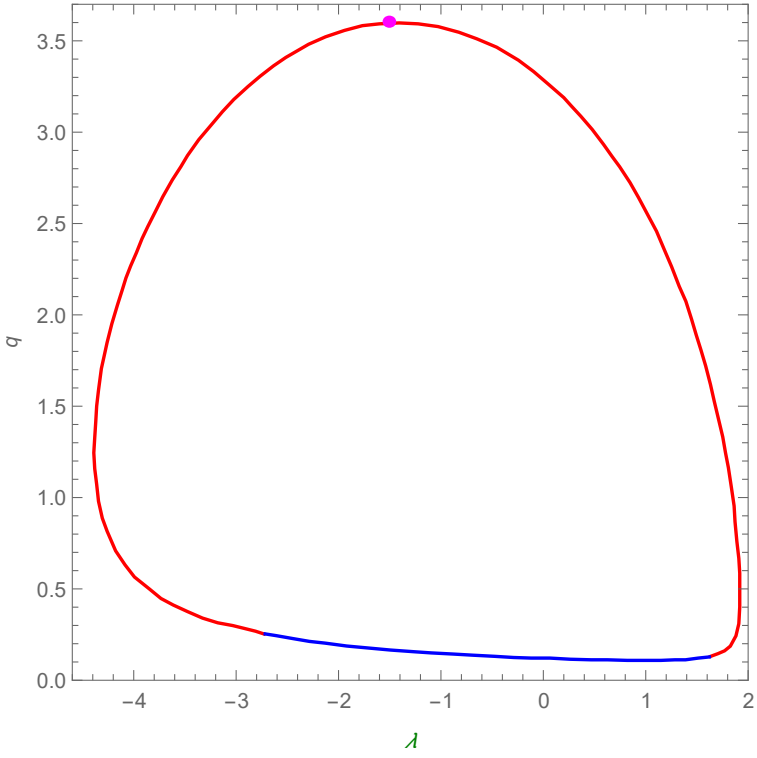

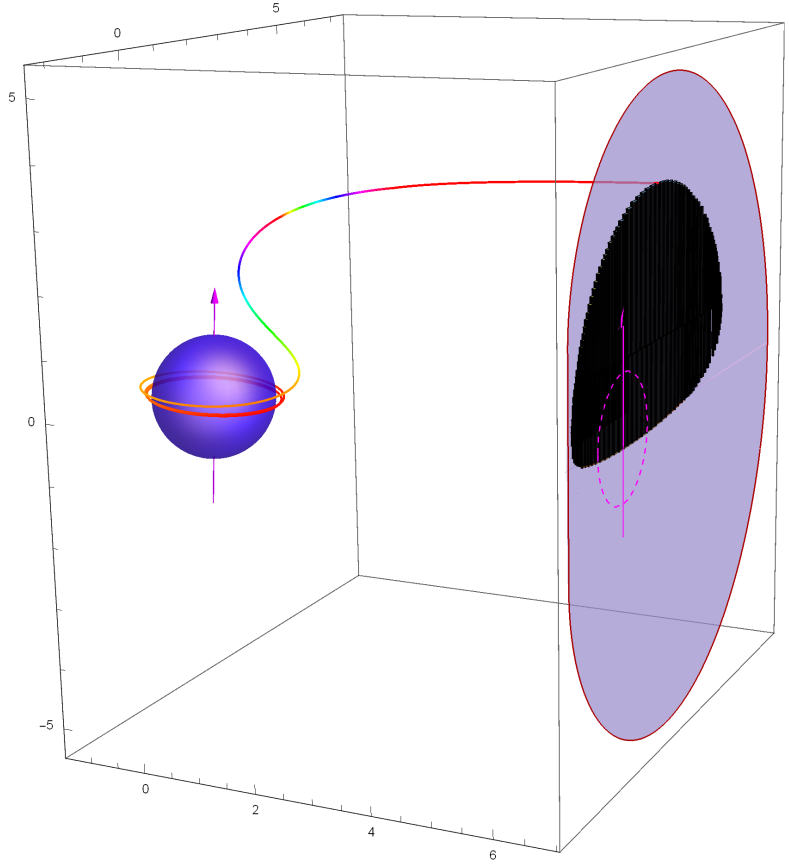

Astrophysical Case 2 : GRMHD accretion simulation

Radiation from both outside and inside photon spheres $r_{\rm ph}$

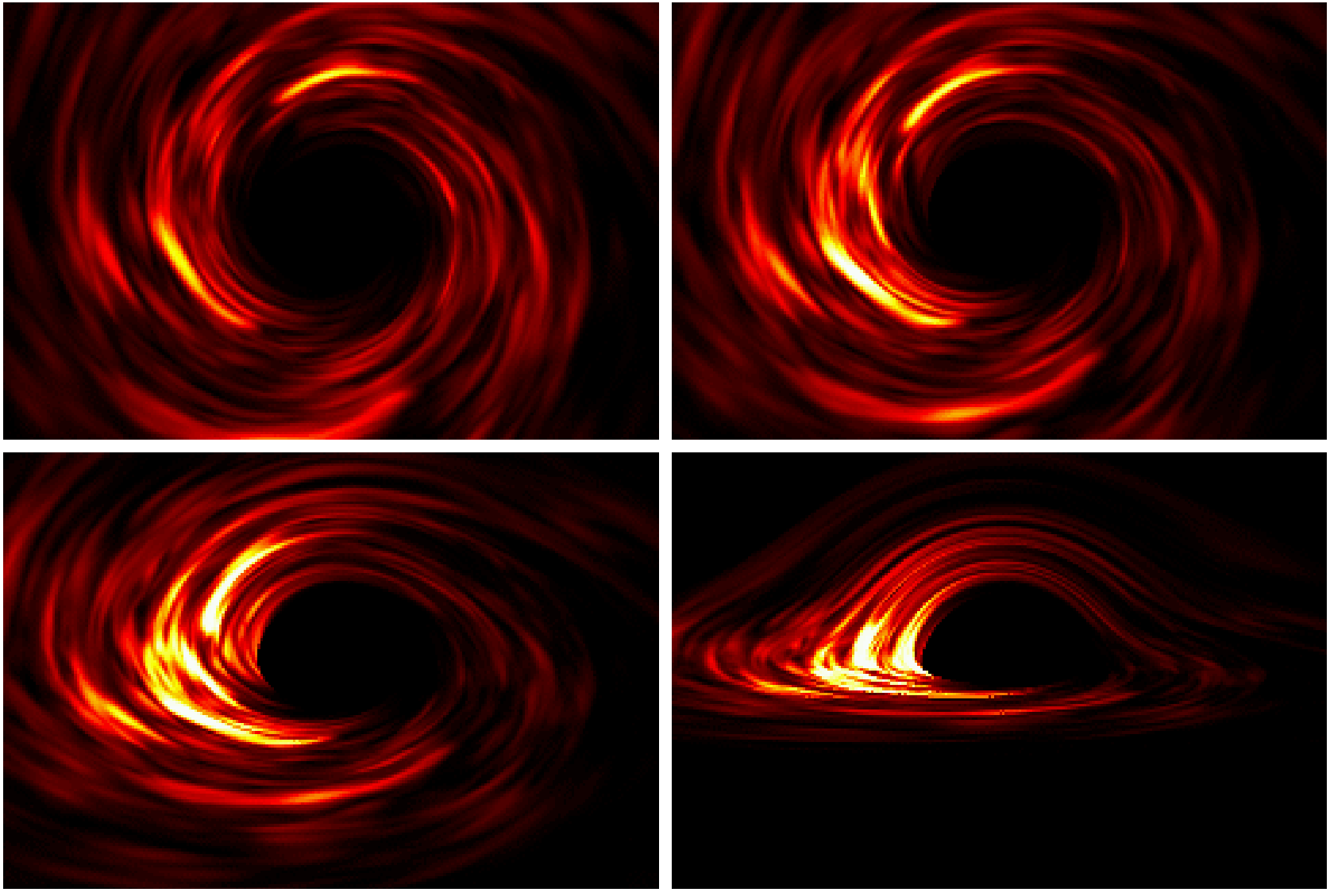

Fe $K\alpha$ line at 6.4 keV

Armitage & Reynolds 2003

Astrophysical Case 2 : Line emission from accretion disk

Radiation from both outside and inside photon spheres $r_{\rm ph}$

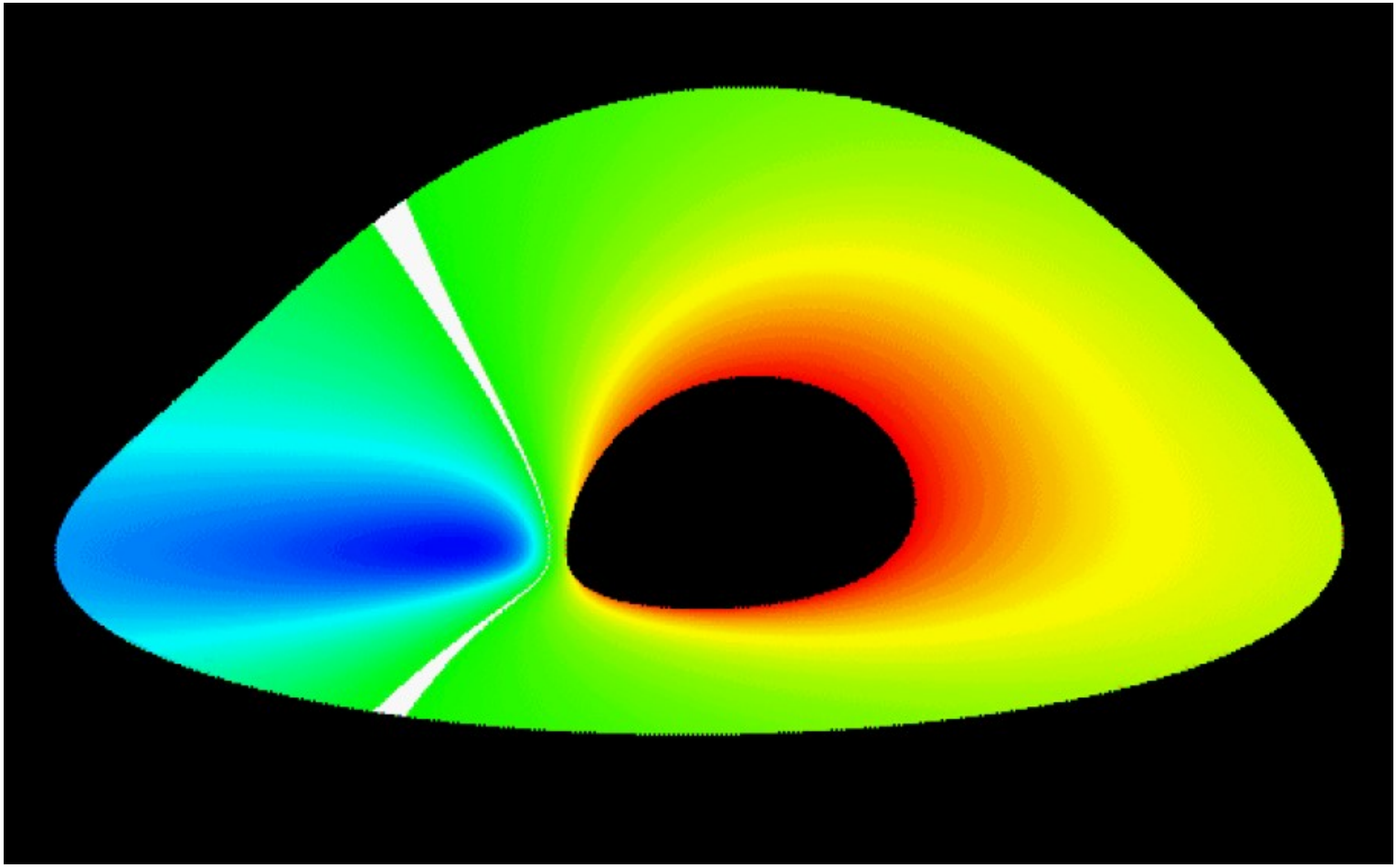

B.C.Bromley, K.Chen, W.A.Miller ApJ **475 57 (1997)**

Right panel: Numerical GRMHD simulation of accretion onto black hole

Hotaka Shiokawa EHT;

https://eventhorizontelescope.org/simulations-gallery

Left panel: Infall of star into black hole: VD and N.O. Nazarova JETP 2019;
https://youtu.be/fps-3frL0AM

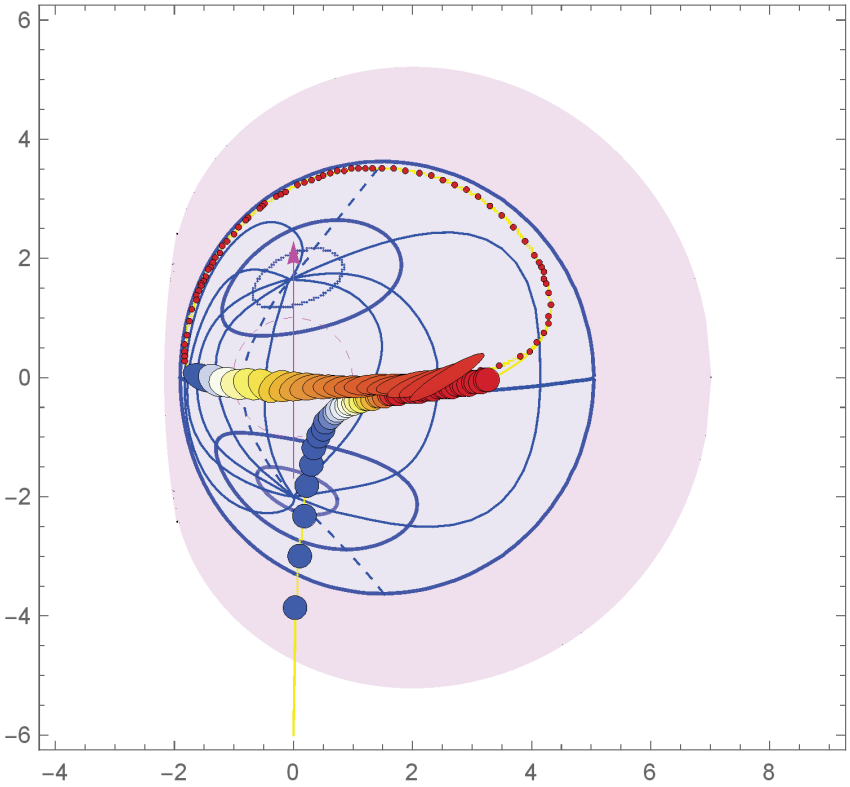

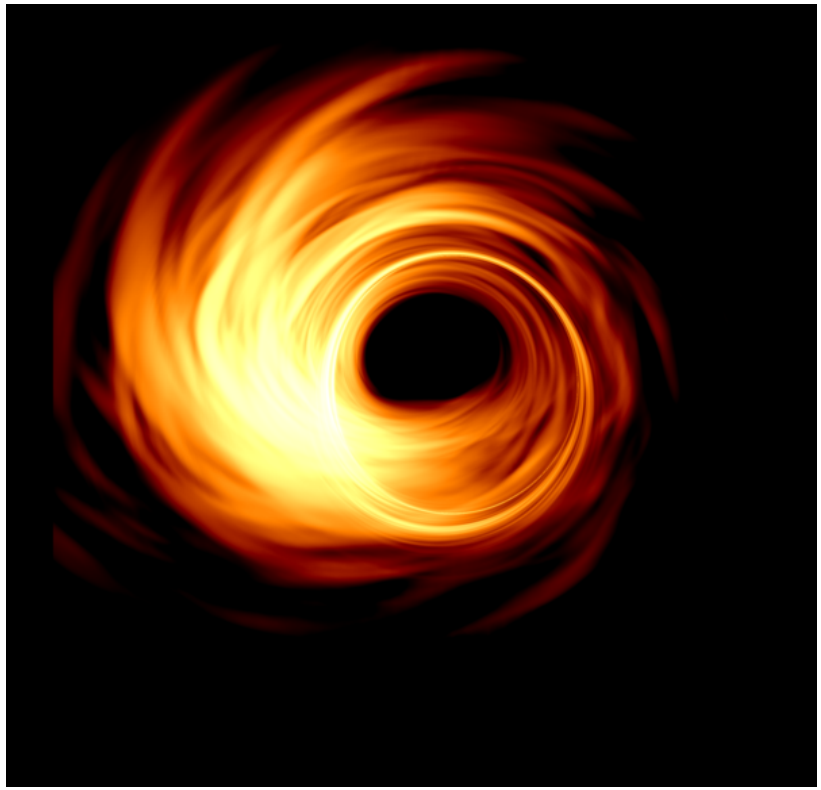

Superposition:

The modeled dark spot and the EHT image of SgrA*

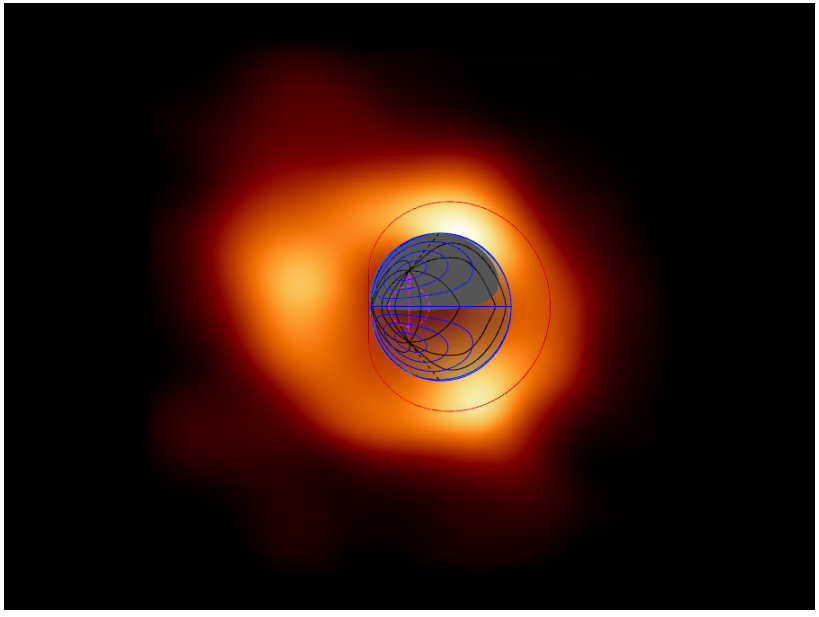

$a = 0.9982$

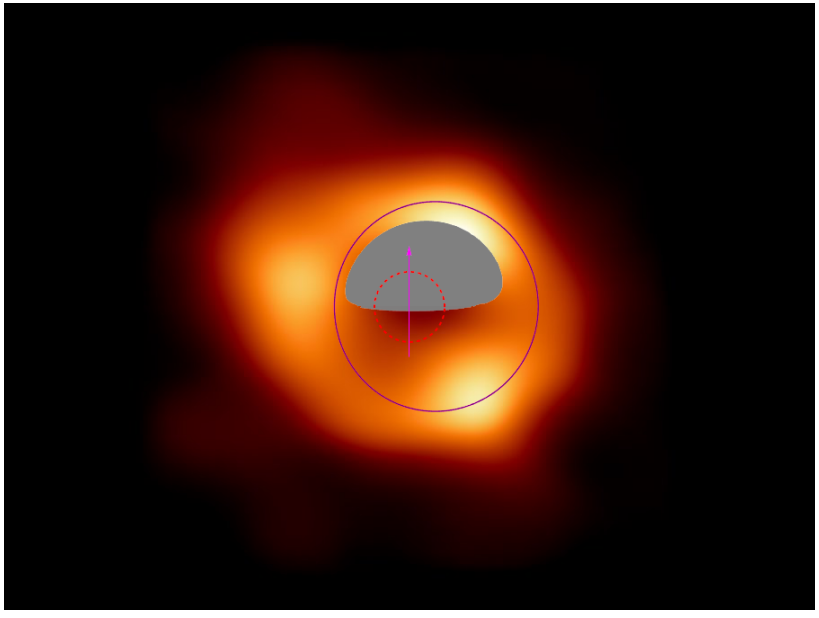

$a = 0.65$

$3D$ picture of M87*, $\theta_0 = 17°$, $a = 1$:

Thin accretion disk and silhouette of the southern hemisphere of event horizon (internal part of the gray closed curve), which is projected inside the awaited position of (invisible) classical black hole shadow at the celestial sphere (purple closed curve)

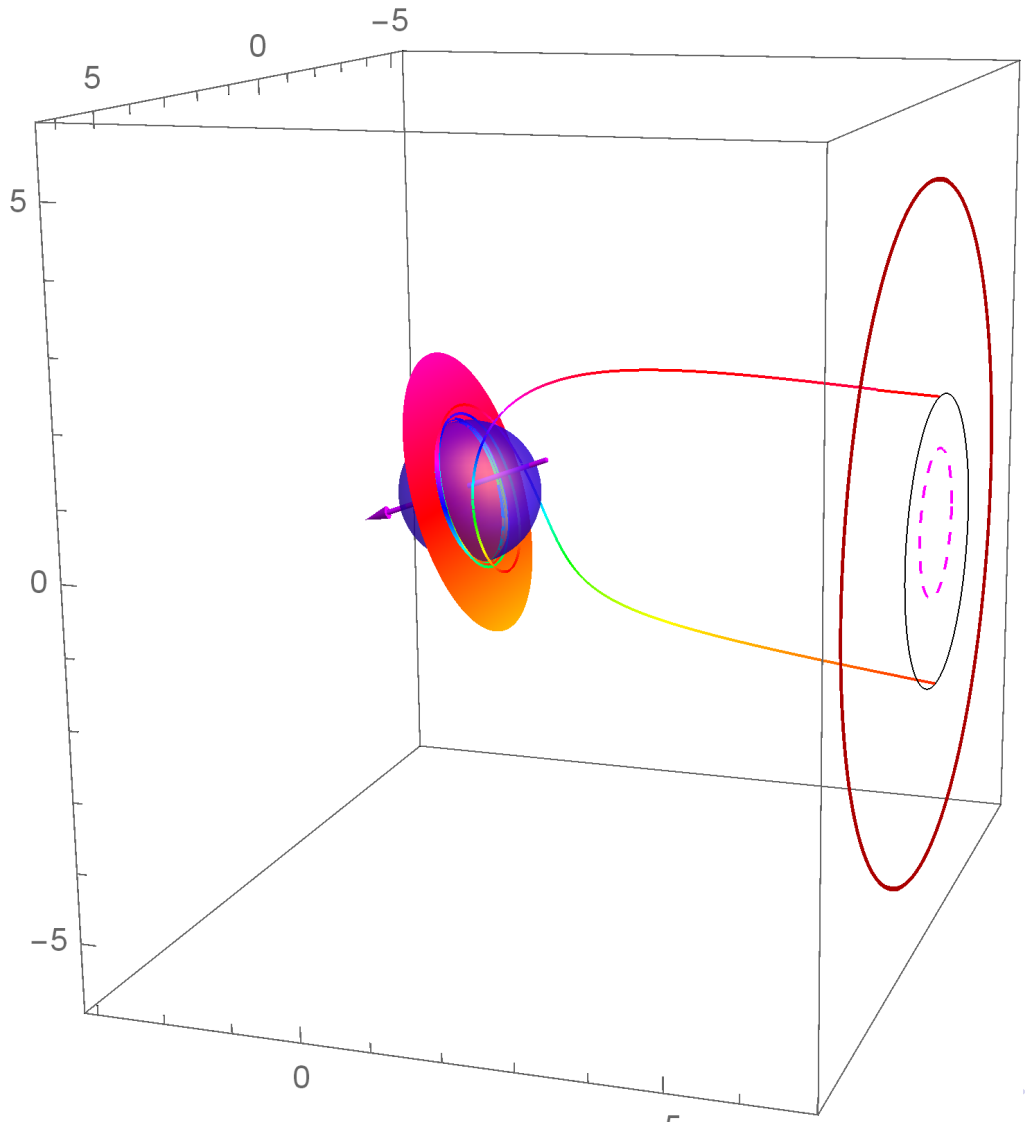

Dark spot in the case of M87* ($\theta_0 = 17°$)

projected inside an outline of the classical black hole shadow

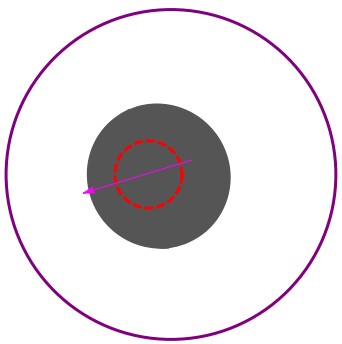

$a = 1$

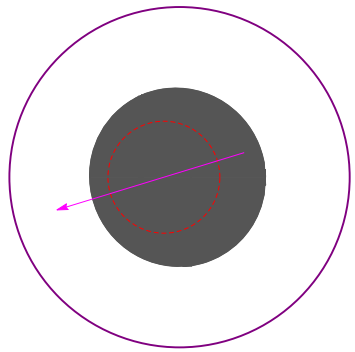

$a = 0.75$

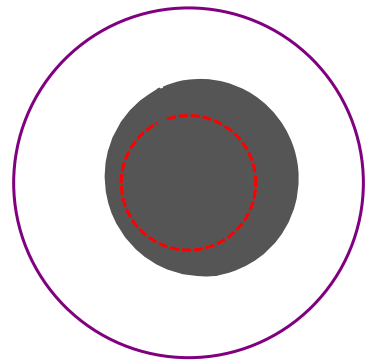

$a = 0$

Dark spot in the case of M87* is a lensed image of the southern hemisphere of the event horizon globe

Superposition: Event Horizon Telescope images and numerically modeled dark spots

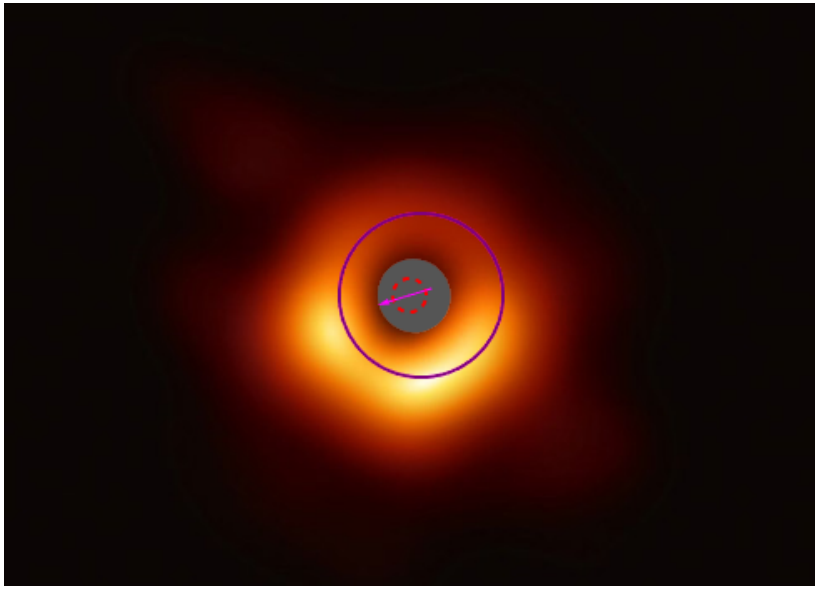

SgrA*: $0.65 \leq a \leq 0.9$

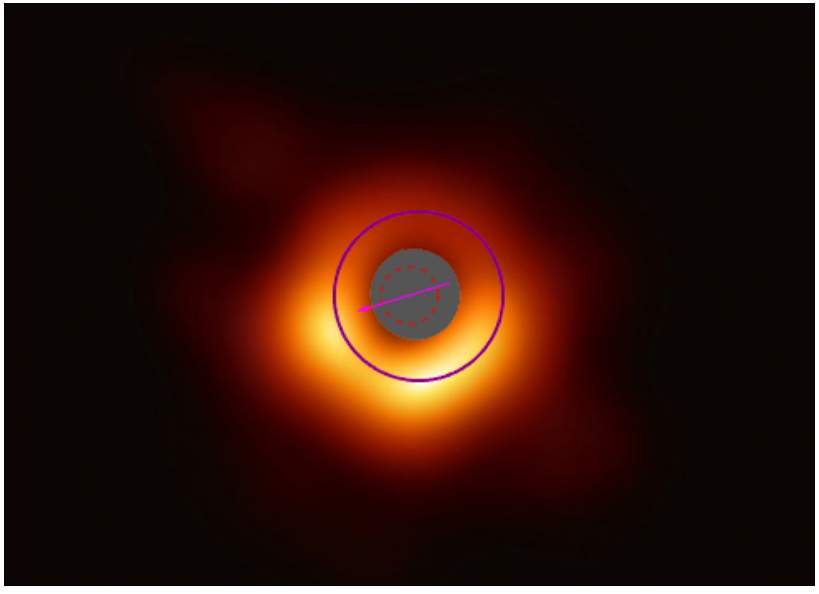

M87*: $0.7 \leq a \leq 1$

Conclusions and Discussions

Observations of black hole images are very crucial for physical interpretation of astrophysical and cosmological observations of the Universe and for understanding the physical origin of enigmatic dark matter and dark energy.

Observations of black hole images opens the unique possibility for verification (or falsification) of modified gravity theories in the strong field limit when gravitation dominates over astrophysical factors

Real verification (or falsification) of modified gravity theories would be possible in the nearest future after construction of the Space Millimetron Observatory with nano-arcsecond angular resolution.

Publication list

- VD / Physical origin of the dark spot at the image of supermassive black hole SgrA* revealed by the EHT collaboration // Astronomy 2022, 1(2), 93–98
- VD, Nazarova, N.O. / Modeling the motion of a bright spot in jets from black holes M87* and SgrA* // Gen. Relativ. Gravit. 53, 83 (2021)
- VD, N.O. Nazarova / Silhouettes of invisible black holes // Physics-Uspekhi 63 (6) 583–600 (2020)
- VD and N. O. Nazarova / Visible shapes of black holes M87* and SgrA* // Universe 2020, 6(9), 154.
- VD, N.O. Nazarova / Event horizon image within black hole shadow // JETP. 128, 578–585 (2019)
- VD and N. O. Nazarova / Brightest point in accretion disk and black hole spin: Implication to the image of black hole M87* // Universe 2019, 5(8), 183
- VD, N. O. Nazarova and V. P. Smirnov / Event horizon silhouette: implications to supermassive black holes M87* and SgrA* // Gen. Relativ. Gravit. (2019) 51: 81
- VD / To see invisible: image of the event horizon within the black hole shadow // IJMPD **28**, No. 13 (2019) 1941005

Image of the object which is not a black hole

ALMA (part of Event Horizon Telescope): Betelgeuse A&A 602, L10 (2017)